LETTER TO THE EDITOR

Structural basis for the gating modulation of Kv4.3 by auxiliary subunits

Cell Research (2022) 32:411–414; https://doi.org/10.1038/s41422-021-00608-4

Dear Editor,

Kv4.3 is an A-type voltage-gated potassium channel that is characterized by fast activation at subthreshold membrane potentials, rapid inactivation, and quick recovery from inactivation.[1] In neurons, Kv4.3 conducts the transient subthreshold somatodendritic A-type potassium current (I_{SA}), knock down of which results in neuropathic pain and epilepsy.[2] In cardiomyocytes, Kv4.3 generates the transient outward potassium current (I_{to}) and its dysfunction is related to a variety of heart diseases, such as hypertrophy, heart failure, myocardial infarction, heart valvular disease, atrial fibrillation, and diabetic cardiomyopathy.[3] Kv4.3 is regulated by accessory subunits Kv Channel-Interacting Proteins (KChIPs) and Dipeptidyl-Peptidase-Like-Proteins (DPLPs). KChIPs are calcium-binding proteins that belong to the neuronal calcium sensor superfamily (NCS). Among four KChIPs (KChIP1–4) in humans, KChIP1 is predominantly expressed in the brain whereas KChIP2 is abundant especially in the heart.[4] DPLPs are type II transmembrane proteins with a large extracellular domain (ECD). Two DPLPs, namely DPP6 and DPP10, have been identified as auxiliary subunits of Kv4.3.[5] KChIPs and DPLPs regulate the gating kinetics, cell surface expression, and subcellular localization of Kv4.3. At present, how KChIPs and DPLPs bind Kv4.3 and regulate its gating properties remains elusive, due to the lack of high-resolution structures of Kv4.3-KChIP and Kv4.3-DPLP complexes.

To verify the modulation of Kv4.3 by KChIP1 or DPP6, we transiently transfected Kv4.3 in HEK293 cells with and without KChIP1 or DPP6 and recorded currents by patch clamp (Supplementary information, Fig. S1a–c). We observed that expression of Kv4.3 alone gave rise to a typical transiently outward current. Notably, co-expression of KChIP1 or DPP6 significantly increased the current density, when compared to Kv4.3 alone (Supplementary information, Fig. S1d–f). Moreover, the activation curves were both significantly left-shifted in co-expressed channels Kv4.3 + KChIP1 and Kv4.3 + DPP6, when compared to Kv4.3 alone (Supplementary information, Fig. S1g, h). The inactivation curve was markedly right-shifted in co-expressed channels Kv4.3 + KChIP1, but left-shifted in co-expressed channels Kv4.3 + DPP6 (Supplementary information, Fig. S1i, j). These results confirmed that KChIP1 and DPP6 regulated the gating properties of Kv4.3.

To reveal the modulation mechanism of Kv4.3 by auxiliary subunits, we first determined the cryo-EM structure of human Kv4.3 alone at 3.0 Å resolution (Fig. 1a; Supplementary information, Fig. S2 and Table S1). Kv4.3 is a homotetrameric channel with dimensions of 80 × 80 × 100 Å (Fig. 1a). Each subunit contains the N-terminal T1 domain (Glu40–Met148), and the transmembrane domain (TMD, Leu163–Arg426) which can be further divided into the S1–S4 voltage-sensing domain (VSD, Leu163–Ser304) and the S5–S6 pore domain (Gln305–Arg426) (Fig. 1a and Supplementary information, Fig. S3a, b). The TMD is arranged in a domain-swapped conformation, where the VSD interacts with S5 from the adjacent subunit (Supplementary information, Fig. S3c). The VSD is in an activated state, with the gating charge residue K299 (K5) pointing to the gating charge transfer center and R290 (R2), R293 (R3), and R296 (R4) above it (Fig. 1b). The pore domain is in an open state, as shown by the over 4 Å van der Waals radius at the activation gate calculated by the HOLE program (Fig. 1c). The T1 domain is located underneath the activation gate and forms direct interactions with four S6 helices (Fig. 1a and Supplementary information, Fig. S3b). In general, Kv4.3 adopts a similar conformation to the Kv1.2–2.1 chimera in the TMD (Fig. 1d and Supplementary information, Fig. S3d).[6] The T1 domain, however, rotates by ~45° in Kv4.3 relative to that in Kv1.2–2.1, likely due to the different lengths and orientations of the linker that connects the T1 domain and VSD (Fig. 1d and Supplementary information, Fig. S3d).

We next determined the structure of the Kv4.3–KChIP1 complex, in co-expression (Kv4.3–KChIP1$_{CE}$) and fusion (Kv4.3–KChIP1$_{Fusion}$) forms at 4.1 Å and 3.4 Å resolution, respectively (Fig. 1e and Supplementary information, Figs. S4, S5 and Table S1). The maps of Kv4.3–KChIP1$_{CE}$ and Kv4.3–KChIP1$_{Fusion}$ align well, suggesting that the fusion expression of Kv4.3 and KChIP1 does not introduce artifact and the higher-resolution structure of Kv4.3–KChIP1$_{Fusion}$ can be used for the analysis of Kv4.3 and KChIP1 interaction (Supplementary information, Fig. S5f). In the structure of Kv4.3–KChIP1$_{Fusion}$, four KChIP1 sit at the periphery of the central tetrameric T1 domain (Fig. 1e). KChIP1 clamps both the N-terminal inactivation ball (Met1–Asp39) of Kv4.3 and a C-terminal helix (Ser470–Thr487, CTH) following S6 from the adjacent subunit, both of which are flexible and not resolved in the structure of Kv4.3 alone (Fig. 1f, g). Kv4 inactivation was proposed to be mediated by cooperative actions of cytoplasmic N-terminal and C-terminal domains.[7] Previous structures of KChIP1 in complex with Kv4.3 T1 domain only revealed interactions between KChIP1 and the N-terminal domain, but not the C-terminal domain.[8,9] Here the Kv4.3–KChIP1$_{Fusion}$ structure shows that KChIP1 slows the initial fast inactivation and accelerates recovery from inactivation of Kv4.3 by sequestering both the N-terminal inactivation ball and the C-terminal helix.

We also determined the structure of the Kv4.3–KChIP2 complex at 2.8 Å resolution (Fig. 1h and Supplementary information, Fig. S6 and Table S1). The interactions of Kv4.3–KChIP1 and Kv4.3–KChIP2 at the N-terminal inactivation ball and C-terminal helix are very similar (Fig. 1f, i). However, in the Kv4.3–KChIP2 complex, the C-terminal end of S6 extends toward the bottom of KChIP2 and forms direct interactions with both KChIP2 and the CTH of Kv4.3, which are not observed in the Kv4.3–KChIP1 complex (Fig. 1g, i). In addition, S6 in the Kv4.3–KChIP2 complex bends by ~15° towards the C-terminal end of the T1 domain in comparison with those in

Received: 12 October 2021 Accepted: 16 December 2021
Published online: 7 January 2022

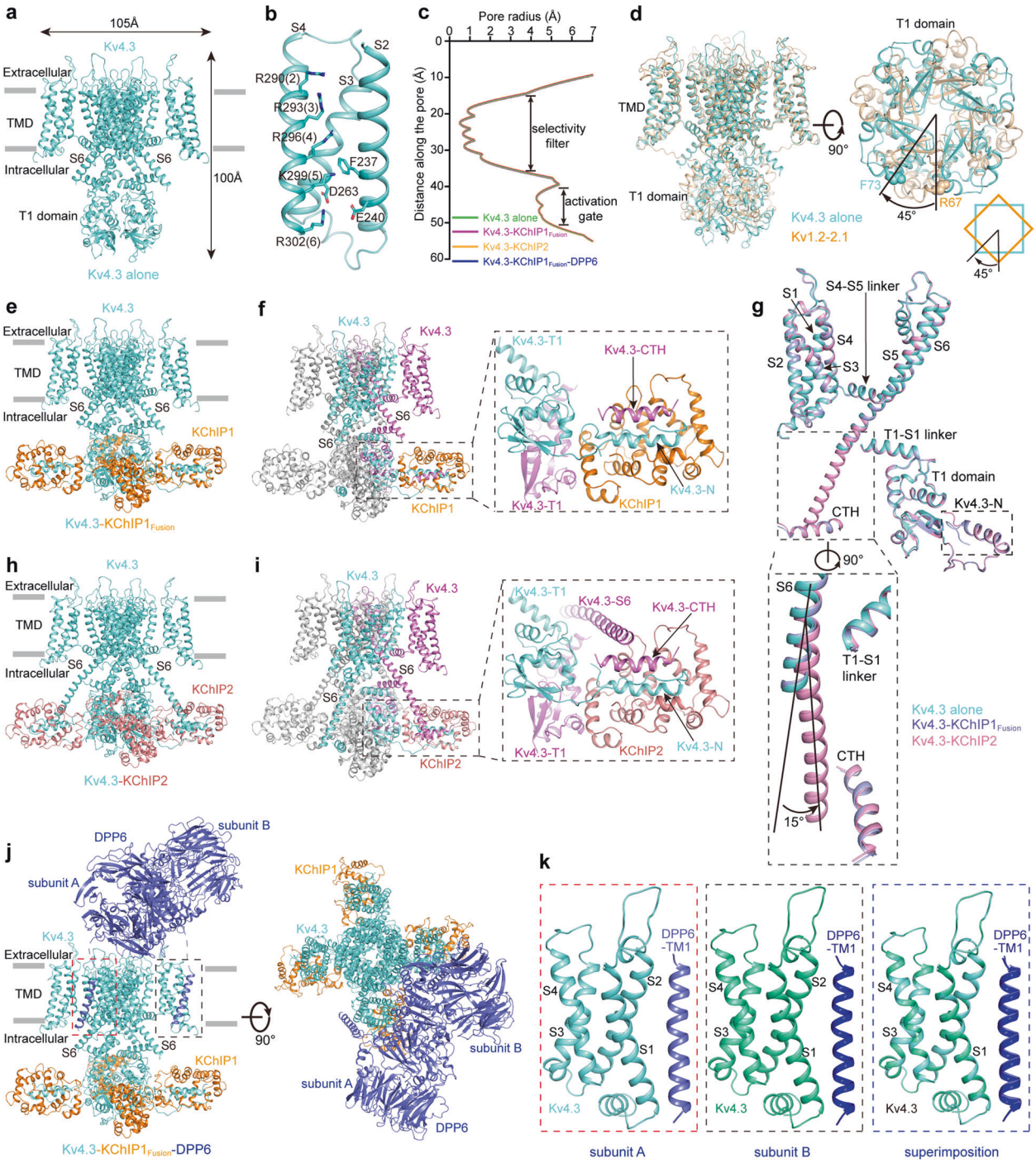

Fig. 1 Structures of Kv4.3. a Side view of the Kv4.3 alone structure. **b** Structure of the VSD in Kv4.3, with S1 omitted for clarity. Side chains of gating charge residues and residues forming the gating charge transfer center are shown as sticks. **c** The van der Waals radii of the pore along the ion-conducting pathway calculated by the HOLE program. **d** Structural superimposition of Kv4.3 and Kv1.2–2.1 chimera (PDB: 2R9R) in side view (left), and bottom view of the T1 domain (right). T1 domain rotates by ~45° in Kv4.3 relative to that in Kv1.2–2.1. **e** Side view of Kv4.3–KChIP1$_{Fusion}$ structure. Kv4.3 is shown in cyan and KChIP1 in orange. **f** Interactions between Kv4.3 N-terminal inactivation ball (Kv4.3-N)/C-terminal helix (Kv4.3-CTH) and KChIP1. Two adjacent subunits of Kv4.3 are shown in cyan and magenta, respectively, and KChIP1 is in orange. **g** Structural superimposition of one subunit of Kv4.3 alone (cyan), Kv4.3–KChIP1$_{Fusion}$ (light blue), and Kv4.3–KChIP2 (pink). In Kv4.3 alone, the flexible N-terminal inactivation ball (Kv4.3-N) and C-terminal helix (Kv4.3-CTH) are invisible, while in Kv4.3-KChIP1$_{Fusion}$ and Kv4.3–KChIP2, they are fixed by KChIP1 or KChIP2. In Kv4.3–KChIP2, the C-terminal end of S6 extends toward the bottom of KChIP2 and forms direct interactions with both KChIP2 and the CTH of Kv4.3, along with a ~15° bending of S6 towards the C-terminal end of T1 domain. **h** Side view of Kv4.3–KChIP2 structure. Kv4.3 is shown in cyan and KChIP2 in pink. **i** Interactions between Kv4.3 N-terminal inactivation ball (Kv4.3-N)/C-terminal helix (Kv4.3-CTH) and KChIP2. Two adjacent subunits of Kv4.3 are shown in cyan and magenta, respectively, and KChIP2 is in pink. **j** Side and top views of Kv4.3–KChIP1$_{Fusion}$–DPP6 structure. Kv4.3 is shown in cyan, KChIP1 is in orange, and DPP6 is in blue. **k** Interactions between DPP6 transmembrane helix (DPP6-TM1) and Kv4.3 VSD in the two adjacent subunits.

Kv4.3 alone and Kv4.3–KChIP1 complex (Fig. 1g). These observations suggest that KChIP2 can also modulate gating of Kv4.3 by directly affecting S6, which is different from KChIP1.

We further determined the structure of the Kv4.3–KChIP1$_{Fusion}$–DPP6 complex at 3.85 Å resolution without applying any symmetry (Fig. 1j and Supplementary information, Fig. S7 and Table S1). In the structure of one channel complex, we only observed two DPP6 molecules, which dimerize at the ECD (Fig. 1j). This ECD dimer is dynamic and the local map quality does not allow us to de novo build the model; yet we were able to fit the previously reported crystal structure of DPP6 ECD dimer into the density (Supplementary information, Fig. S7e).[10] While the ECD dimer does not interact with Kv4.3 at the extracellular side, the transmembrane helices (TM1) of the DPP6 dimer forms hydrophobic interactions with the N-terminal ends of both S1 and S2 in the VSDs from the adjacent two subunits of Kv4.3 (Fig. 1j, k). Although there are only two DPP6 subunits in the Kv4.3–KChIP1$_{Fusion}$–DPP6 complex, the C4 symmetry of Kv4.3 is not destroyed by the asymmetric binding of DPP6. And interactions of DPP6 TM1 and Kv4.3 VSD are essentially the same between the adjacent two subunits (Fig. 1k). Upon membrane potential depolarization, S4 in Kv4.3 undergoes upwards translational motion while S1 and S2 remain almost static.[6] The binding of DPP6 here further stabilizes S1 and S2 and likely enhances the channel's voltage sensitivity, which can explain why DPLPs are able to modulate Kv4.3 gating by shifting the voltage dependence of activation and inactivation toward more negative membrane potentials.[11]

In summary, in this study, we have determined four structures of Kv4.3, namely Kv4.3 alone, Kv4.3–KChIP1$_{Fusion}$, Kv4.3–KChIP2, and Kv4.3–KChIP1$_{Fusion}$–DPP6. This study reveals interactions between Kv4.3 and KChIP1, between Kv4.3 and KChIP2, and between Kv4.3 and DPP6, providing structural insights into the modulation mechanism of Kv4.3 by auxiliary subunits. In all four structures, the TMDs of Kv4.3 are in the same conformation, with VSDs in an activated state and the activation gates in an open conformation (Fig. 1c). The open activated gate is filled up with tubular-shaped density, which may arise from lipid or detergent molecules (Supplementary information, Fig. S3e).

During our manuscript preparation, a similar structural study on another potassium channel Kv4.2 was published in *Nature*.[12] The structure arrangements of Kv4.3–KChIP–DPP6 and Kv4.2–KChIP1–DPP6S complexes are very similar: they share the same interactions between Kv4 and KChIP, and between Kv4 and DPP6. However, there are two major differences between Kv4.3 and Kv4.2 complexes. First, in the Kv4.2–KChIP1 complex, the S6 is exceptionally long and its C-terminus extends to the bottom of the complex, which is similar to the S6 in Kv4.3–KChIP2 complex, but different from the S6 in Kv4.3–KChIP1 complex (Fig. 1f, g, i). In the Kv4.3-KChIP1 complex, the S6 remains the same short as that in Kv4.3 alone (Fig. 1a, f, g). This difference is not introduced by the fusion expression of Kv4.3–KChIP1 because in both Kv4.3–KChIP1$_{Fusion}$ and Kv4.3–KChIP1$_{CE}$ structures we observe the same short S6 (Supplementary information, Fig. S5f). Second, in the Kv4.2–KChIP1–DPP6S structure, complexes with either four DPP6S or two DPP6S (a short isoform of DPP6) molecules were captured, while in the Kv4.3–KChIP1$_{Fusion}$–DPP6 structure only complexes with two DPP6 molecules were identified (Fig. 1j). These two structural differences may be ascribed to the difference between Kv4.3 and Kv4.2 and (or) the difference between DPP6 and DPP6S. Nevertheless, the structural comparison of Kv4.3–KChIP–DPP6 and Kv4.2–KChIP1–DPP6S complexes implicates the conservation and divergence of the gating mechanisms of Kv4. The structural studies of Kv4.3–KChIP–DPP6 and Kv4.2–KChIP1–DPP6S together provide insights into the complex gating modulation of Kv4 by different auxiliary subunits.

Demin Ma[1,2,7], Cheng Zhao[1,7], Xiaochen Wang[3], Xiaoxiao Li[1], Yi Zha[1], Yan Zhang[1], Guosheng Fu[2], Ping Liang[3]✉, Jiangtao Guo[1,2,4,5,6]✉ and Dongwu Lai[2]✉

[1]*Department of Biophysics, and Department of Pathology of Sir Run Run Shaw Hospital, Zhejiang University School of Medicine, Hangzhou, Zhejiang, China.* [2]*Department of Cardiology, Key Laboratory of Cardiovascular Intervention and Regenerative Medicine of Zhejiang Province, Sir Run Run Shaw Hospital, Zhejiang University School of Medicine, Hangzhou, Zhejiang, China.* [3]*Key Laboratory of Combined Multi-organ Transplantation, Ministry of Public Health, the First Affiliated Hospital, and Institute of Translational Medicine, Zhejiang University School of Medicine, Hangzhou, Zhejiang, China.* [4]*State Key Laboratory of Plant Physiology and Biochemistry, College of Life Sciences, Zhejiang University, Hangzhou, Zhejiang, China.* [5]*Cancer Center, Zhejiang University, Hangzhou, Zhejiang, China.* [6]*Liangzhu Laboratory, Zhejiang University Medical Center, Hangzhou, Zhejiang, China.* [7]*These authors contributed equally: Demin Ma, Cheng Zhao.*
✉*email: pingliang@zju.edu.cn; jiangtaoguo@zju.edu.cn; laidw@zju.edu.cn*

DATA AVAILABILITY

The cryo-EM density maps of Kv4.3 alone, Kv4.3–KChIP1$_{Fusion}$, Kv4.3–KChIP2, and Kv4.3–KChIP1$_{Fusion}$–DPP6 have been deposited in the Electron Microscopy Data Bank (EMDB) under accession numbers EMD-32296, EMD-32330, EMD-32334, and EMD-32335, respectively. The coordinates of Kv4.3 alone, Kv4.3–KChIP1$_{Fusion}$, Kv4.3–KChIP2, and Kv4.3–KChIP1$_{Fusion}$–DPP6 have been deposited in the RCSB Protein Data Bank (PDB) under accession codes 7W3Y, 7W6N, 7W6S, and 7W6T, respectively.

REFERENCES

1. Zemel, B. M., Ritter, D. M., Covarrubias, M. & Muqeem, T. *Front. Mol. Neurosci.* **11**, 253 (2018).
2. Kuo, Y. L. et al. *J. Neurosci.* **37**, 4391–4404 (2017).
3. Huo, R., Sheng, Y., Guo, W. T. & Dong, D. L. *Channels* **8**, 203–209 (2014).
4. An, W. F. et al. *Nature* **403**, 553–556 (2000).
5. Cheng, C. F. et al. *J. Comp. Neurol.* **524**, 846–873 (2016).
6. Long, S. B., Tao, X., Campbell, E. B. & MacKinnon, R. *Nature* **450**, 376–382 (2007).
7. Jerng, H. H. & Covarrubias, M. *Biophys. J.* **72**, 163–174 (1997).
8. Pioletti, M., Findeisen, F., Hura, G. L. & Minor, D. L. *Nat. Struct. Mol. Biol.* **13**, 987–995 (2006).
9. Wang, H. Y. et al. *Nat. Neurosci.* **10**, 263–263 (2007).
10. Strop, P., Bankovich, A. J., Hansen, K. C., Garcia, K. C. & Brunger, A. T. *J. Mol. Biol.* **343**, 1055–1065 (2004).
11. Nadal, M. S. et al. *Neuron* **37**, 449–461 (2003).
12. Kise, Y. et al. *Nature* **599**, 158–164 (2021).

ACKNOWLEDGEMENTS

Single-particle cryo-EM data were collected at the Center of Cryo-Electron Microscopy at Zhejiang University. We thank Dr. Xing Zhang and Dr. Shenghai Chang for the support in granting facility access and data acquisition. This work was supported in part by the Ministry of Science and Technology of China (2020YFA0908501 and 2018YFA0508100 to J.G., and 2017YFA0103700 to P.L.), the National Natural Science Foundation of China (31870724 to J.G., 81974025 to D.L., and 81922006 to P.L.), Zhejiang Provincial Natural Science Foundation (LR19C050002 to J.G., LY19H020007 to D.L.), and the Fundamental Research Funds for the Central Universities (2021FZZX001-28 to J.G., and LD21H020001 to P.L.). J.G. is supported by MOE Frontier Science Center for Brain Science & Brain-Machine Integration, Zhejiang University.

AUTHOR CONTRIBUTIONS

J.G., D.L., P.L., and G.F. conceived and supervised the project. D.M., C.Z., X.L., Y.Zha, and Y.Zhang prepared the samples, performed data acquisition, structure determination, and data analysis. X.W. and P.L. performed the electrophysiology assays. All authors participated in the data analysis and manuscript preparation.

COMPETING INTERESTS

The authors declare no competing interests.

ADDITIONAL INFORMATION

Supplementary information The online version contains supplementary material available at https://doi.org/10.1038/s41422-021-00608-4.

Correspondence and requests for materials should be addressed to Ping Liang, Jiangtao Guo or Dongwu Lai.